Title

Resonance Raman Spectroscopy and Electron–Phonon Coupling in Zinc Selenide Quantum Dots

Journal

The Journal of Physical Chemistry C, 120(51)

ISSN

1932-7447

Authors

Gong, Ke
Kelley, David F
Kelley, Anne Myers

Publication Date

2016-12-29

DOI

10.1021/acs.jpcc.6b12202

Resonance Raman Spectroscopy and Electron-Phonon Coupling in Zinc Selenide Quantum Dots

Ke Gong, David F. Kelley, and Anne Myers Kelley*

Chemistry & Chemical Biology, University of California, Merced, 5200 North Lake Road, Merced, CA 95343

*Author to whom correspondence should be addressed; amkelley@ucmerced.edu

Abstract

Resonance Raman spectra, including absolute scattering cross-sections, depolarization ratios, and overtone to fundamental intensity ratios, have been measured for three sizes of ZnSe quantum dots between 3.8 and 4.9 nm diameter (first excitonic peak maximum at 402 to 417 nm) using excitation wavelengths between 400 and 425 nm. Spectra were obtained both in cyclohexane solution and in thin films in order to quantitate the exciton-phonon coupling strength. The Raman data and optical absorption spectra were simulated using a particle in a sphere effective mass model for the excitonic transitions similar to that previously employed for CdSe [C. Lin, K. Gong, D. F. Kelley, and A. M. Kelley, J. Phys. Chem. C **119**, 7491 (2015)]. The Huang-Rhys parameter of the longitudinal optical phonon in the lowest excitonic transition is in the range S = 0.3 to 0.5, about a factor of two larger than for CdSe quantum dots of similar size. Smaller ZnSe quantum dots (~3.0 nm diameter, first excitonic maximum at 379 nm) measured in films show stronger overtones, suggesting an increase in Huang-Rhys parameter at smaller sizes.

Introduction

Spherical nanocrystals (quantum dots) of the Zn, Cd, and Pb chalcogenides (S, Se, and Te) have been studied widely both for fundamental interest and because of a number of current or potential applications. Cadmium selenide has a bulk optical band gap that is in the far red spectral region. Quantum confinement imposed by reducing the size allows the lowest-energy optical transition of CdSe nanostructures to be tuned throughout the visible range. Because of the optical properties and the relative ease of synthesizing highly luminescent, monodisperse particles, the spectroscopic and photophysical properties of CdSe nanocrystals have been studied in great detail both experimentally and theoretically. Great effort has been put into developing synthetic methods that produce nearly homogeneous samples that are highly crystalline and have few defects. The bulk band gap of zinc selenide is at about 460 nm, so nanocrystals of this material absorb and emit in the violet to near-UV range. Accordingly, ZnSe nanocrystals have fewer applications in imaging and optoelectronics and they have not been studied as thoroughly as CdSe. Nevertheless, comparison of the spectroscopic and photophysical properties of ZnSe and CdSe is potentially enlightening for the insight it provides to our fundamental understanding of the optical transitions in quantum dots.

CdSe and ZnSe quantum dots of the sizes typically studied experimentally have several hundred to many thousands of atoms and are too large to be handled routinely with high-level atomistic electronic structure methods such as density functional theory, although such methods are widely applied to smaller clusters. Rather, calculations on quantum dots of this size are often carried out by using an empirical force field to calculate the ground-state geometry and phonon modes,[1] and a particle in a sphere effective mass approximation (EMA) model to calculate the excitonic energies and wavefunctions.[2-4] We have employed these models in previous studies

aimed at understanding the electron-phonon coupling in CdSe quantum dots and how it depends on size and/or the presence of a CdS shell.[5,6] This coupling is thought to be dominated by the Fröhlich interaction, in which the electric field of the conduction band electron and valence band hole interact with the polar crystal. Simple EMA models predict that the electron-phonon coupling (EPC) should decrease with increasing QD size and should increase strongly upon adding a "type-1 ½" or "quasi-type-II" CdS shell to a CdSe QD.[5,6] However, the experimental results contradict both expectations. For this reason, we set out to measure EPC in a different but closely related QD system, ZnSe.

In cadmium and zinc selenides, the orbitals that make up the top of the valence band (the low-energy hole states) are composed mainly of Se 4p orbitals while the orbitals at the bottom of the conduction band (the low-energy electron states) consist mainly of the s orbitals on Cd or Zn. Thus we expect that many aspects of the electronic structure should be similar, including the fine structure of the excitonic transitions that arises from the valence band degeneracy.[2,7,8] The phonon dispersion curves of the bulk materials are also quite similar apart from the generally higher frequencies in the lighter ZnSe (the highest-frequency longitudinal optical phonon is at about 250 cm^{-1} in ZnSe and 210 cm^{-1} in CdSe).[9,10] However, ZnSe is less polar than CdSe based on atomic charges inferred from bulk electroelastic properties,[11] suggesting that the Fröhlich coupling of the excitonic charge distribution to the polar optical phonons might be weaker.

In this paper we report a quantitative analysis of the resonance Raman spectra of ZnSe QDs in solution to evaluate this hypothesis. Specifically, we analyze the absolute resonance Raman scattering cross-section for the longitudinal optical (LO) phonon, its Raman depolarization ratio, and its overtone to fundamental intensity ratio, together with the absorption spectrum, to estimate the Huang-Rhys parameter (S) for the LO phonon in the lowest excitonic transition of ZnSe

QDs. The Huang-Rhys parameter is given by $S = \Delta^2/2$, where Δ is the equilibrium displacement along the phonon mode in the excited electronic state, measured in units of the harmonic oscillator dimensionless normal coordinate. The Huang-Rhys parameter is therefore a quantitative measure of the extent to which the electronic excitation couples to the phonon motion, the exciton-phonon coupling (EPC). Four sizes of ZnSe QDs are examined, spanning about the same size range explored in our previous work on CdSe.[5] To our knowledge no resonance Raman spectra of ZnSe QDs have been published previously, and only a few nonresonant (visible excitation) spectra of colloidal ZnSe QDs have been reported.[12,13] We discuss these results in comparison to the corresponding analyses of CdSe.[5,14]

Experimental section

A. Chemicals

Zinc stearate (Alfa Aesar, ZnO 12.5-14%), 1-octadecene (Aldrich, technical grade, 90%), Se powder (Alfa Aesar, 200 mesh, 99.999%), toluene (Alfa Aesar, ACS, 99.5%), cyclohexane (Acros Organics, spectrophotometric grade, 99+%), and hexadecanethiol (Sigma-Aldrich, >95%) were used as received. Methanol (Acros Organics, 99+% extra pure) was distilled over iodine-activated magnesium before use.

B. Synthesis of ZnSe quantum dots (QDs)

Zincblende ZnSe QDs were synthesized using a modification of the procedure described in ref. 15. Zinc stearate (0.0632 g, 0.1 mmol) and 1-octadecene (5 mL) were loaded into a 25 mL three-neck flask, evacuated and filled with nitrogen. The temperature was then raised to ~305 °C. In an empty vial, Se powder (0.0039 g, 0.05 mmol) was dispersed in 1-octadecene (1 mL)

by sonication for 2 min and injected into the above flask. After the injection, the reaction temperature was held at 280 °C for 1-3 min, which yielded ZnSe QDs with their first exciton absorbance between 373 and 382 nm. To further grow the ZnSe particles, zinc stearate in warm ODE was added dropwise into the reaction mixture at 230 °C - 240 °C. The reaction was stopped after 10-30 minutes, depending on the desired size, by cooling down to room temperature. The QDs were extracted into cyclohexane and then washed several times by precipitation with methanol, centrifuged, and redissolved in cyclohexane.

C. Resonance Raman spectroscopy

Resonance Raman spectra and absolute Raman cross-sections were measured using the instrumentation and general methods described in our previous work,[5,14] with the following modifications. Excitation wavelengths between 382 and 425 nm were obtained from a frequency-doubled picosecond Ti:sapphire laser (Spectra-Physics Tsunami) producing pulses of 1-2 ps duration at a repetition rate of 82 MHz. The focused laser power at the sample was about 10^4 W/cm^2. For solution phase Raman measurements, the QDs were dissolved in cyclohexane. Cyclohexane was used instead of chloroform to avoid spectral interferences with the Raman lines of ZnSe. The windows of the fused silica cuvettes used for the solution phase experiments have a broad Raman band with a maximum near 500 cm^{-1} which interferes with the overtone of the ZnSe LO phonon. Therefore, the solution phase spectra were used for determination of the absolute Raman cross-sections and depolarization ratios for the LO fundamental while the LO overtone to fundamental ratio was obtained from spectra of samples deposited onto aluminum substrates by drop-casting from cyclohexane with hexadecanethiol added as a hole quencher.[14] All samples were translated along one axis during Raman data collection to avoid local heating or photochemistry. For each spectrum, 20 to 60 exposures of 1 to 2 minutes each were averaged.

Absolute cross sections were obtained relative to those previously determined for cyclohexane.[16] For excitation wavelengths longer than 400 nm, the standard 10x microscope objective was used for excitation and collection of the backscattered Raman signal, and a film polarizer was placed in the scattered beam while the polarization of the excitation beam was switched between parallel and perpendicular using a Soleil-Babinet compensator. The wavelength-dependent transmission of both the objective and the polarizer was corrected for by measuring the fluorescence spectrum of anthracene and comparing to literature spectra.

For each of the three largest sizes of QDs, spectra were obtained at two different excitation wavelengths within the first excitonic transition both in cyclohexane solution and in thin films. Because we were not able to obtain reliable values for the absorption cross-section of the smallest QDs (see below and Supporting Information), no analysis could be performed on the solution-phase data. Only thin-film spectra, obtained using a 40x uv-optimized objective, are reported for the smallest QDs. The photoluminescence from these samples was relatively weak (estimated quantum yield << 0.1) but still produced a significant background on the resonance Raman spectra. The photoluminescence backgrounds were fit to a smooth function and subtracted from the displayed Raman spectra.

Results

A. Determination of molar absorptivity

Quantitative analysis of resonance Raman intensities requires knowledge of the absorption cross-section or molar absorptivity ($\sigma_A=3.826\text{x}10^{-5}\varepsilon$ where ε is the molar absorptivity in M^{-1} cm^{-1} and σ_A is the cross-section in $Å^2$). It is needed to determine the concentration of the QDs in the solution phase spectra such that the absolute scattering cross-sections can be obtained from the

ratio of ZnSe to cyclohexane integrated Raman intensities. It is also needed for the calculations that model the Raman cross-sections to determine the EPC. Raman intensities on resonance with a single excitonic transition depend on three factors: the transition dipole moment (which determines the radiative rate of the excited state), the excitonic dephasing rate (which determines how quickly the sharp Raman-like emission is converted to broad fluorescence), and the EPC (which determines how the sharp emission is partitioned between Rayleigh scattering and the various Raman transitions).[17-19] The transition dipole moment, which can be obtained from the integrated molar absorptivity, is needed so that the other two factors can be determined from the resonance Raman cross-sections for the fundamental and first overtone.

Direct determination of molar absorptivities of QDs is straightforward in principle but technically quite demanding to do accurately,[20] and apparently no molar absorptivities have been published for ZnSe QDs. We therefore estimated the peak molar absorptivity of the lowest excitonic transition of our QDs using two different approaches. The first assumes that the transition dipole moment for the lowest excitonic transition of ZnSe QDs is the same as for CdSe QDs with the same quantum confinement energy. The second assumes that the absorption coefficient on a per unit cell basis is the same for bulk ZnSe and for ZnSe QDs at sufficiently high photon energies, here taken to be 4.0 eV (310 nm),[21] scaled by the appropriate local field factor.[22] Both approaches yield similar values for the peak molar absorptivity (absorption cross-section) for the three larger QDs, but the two methods deviate considerably for the smallest size absorbing at 379 nm. The 310 nm absorption is likely to be affected by quantum confinement when the particles are very small and the first exciton absorbs below 400 nm. We therefore used the values obtained from the first method, but refrained from carrying out any analyses that

require knowledge of the absorptivity for the smallest size QDs. The calculations and the resulting peak molar absorptivities are detailed in the Supporting Information.

Figure 1 shows the absorption spectra, in units of absorption cross-section, for the four sizes of ZnSe QDs. The sizes were estimated by interpolation of the data from refs. 23 and 8, as discussed in the Supporting Information.

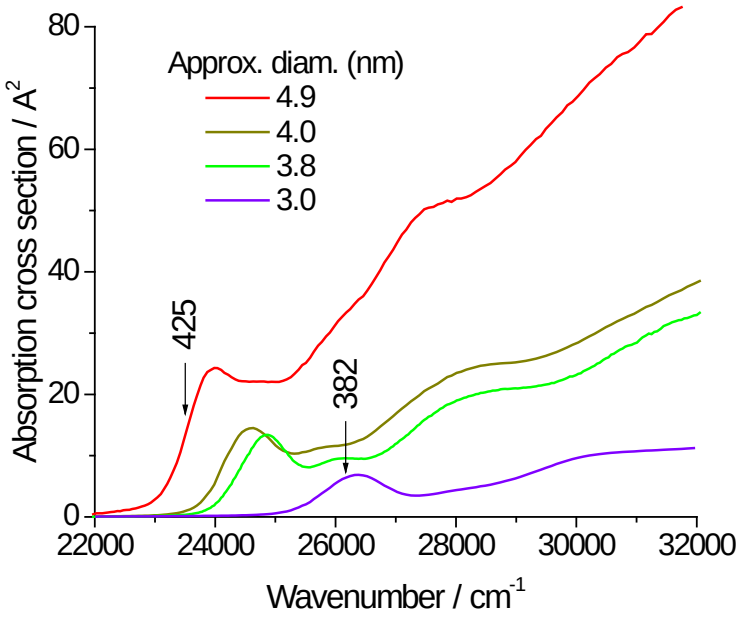

Figure 1. Optical absorption spectra of the four sizes of ZnSe QDs and the highest and lowest wavelength used for Raman excitation.

B. Resonance Raman spectra

Figure 2 shows the resonance Raman spectra of each of the three larger QD samples in cyclohexane at one excitation wavelength. All of the spectra are strongly but not completely polarized (depolarization ratio ~0.2), indicating some deviation from perfect spherical symmetry as discussed in refs. 5 and 14. Figure 3 shows the spectra of all four sizes obtained from dried films on aluminum. The dominant feature in the spectra is the fundamental of the "longitudinal

optical" (LO) phonon of ZnSe, which has a maximum at 250 ± 1 cm^{-1} in all four samples. There is a weak shoulder at lower frequencies, similar to the corresponding LO phonon region of CdSe.[24] The bulk LO frequency at the Γ point is 253 cm^{-1},[9] and the ~3 cm^{-1} downshift in 3-5 nm QDs is similar to that observed in CdSe.[25] There is also a fairly strong peak corresponding to the first overtone of the LO phonon, which appears as a broad band with its maximum at 498-501 cm^{-1}, indicating very little anharmonicity. The second (three quanta) overtone is weakly visible at ~750 cm^{-1} but no attempt was made to use its intensity quantitatively. Table 1 summarizes the absolute resonance Raman cross sections, depolarization ratios, and overtone to fundamental intensity ratios for both samples at both excitation wavelengths.

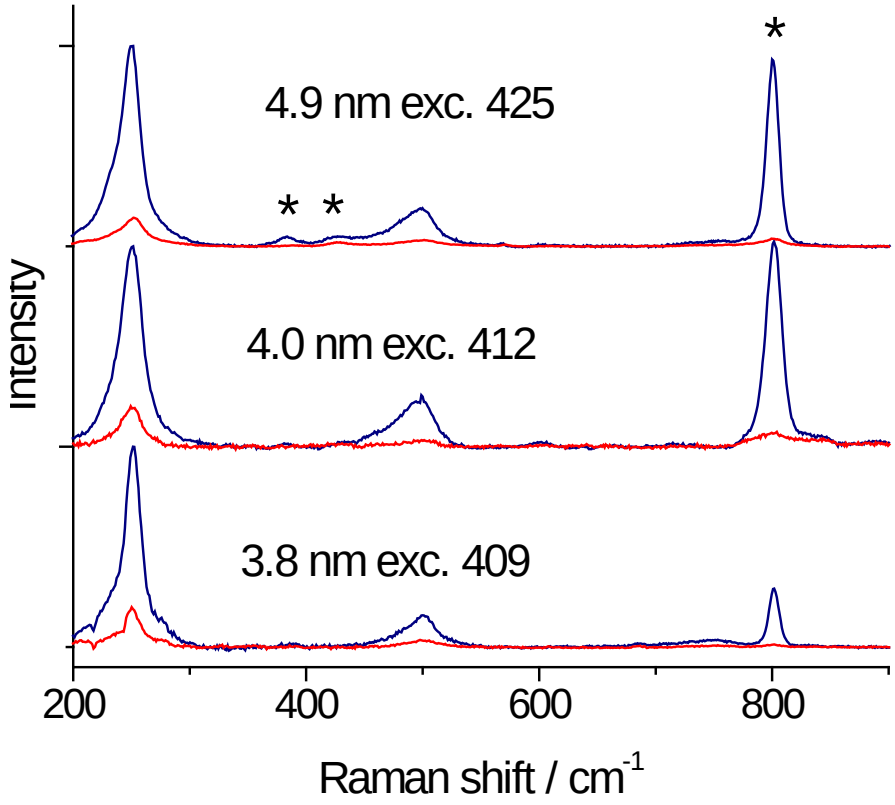

Figure 2. Resonance Raman spectra of the three largest sizes of ZnSe QDs in cyclohexane solution at the indicated excitation wavelengths. Parallel (navy) and perpendicular (red) polarizations are shown. Asterisks label cyclohexane peaks. Spectra are scaled to a common maximum and displaced. Concentrations are 0.85, 3.13, and 14.8 μM for the 4.9, 4.0, and 3.8 nm QDs, respectively.

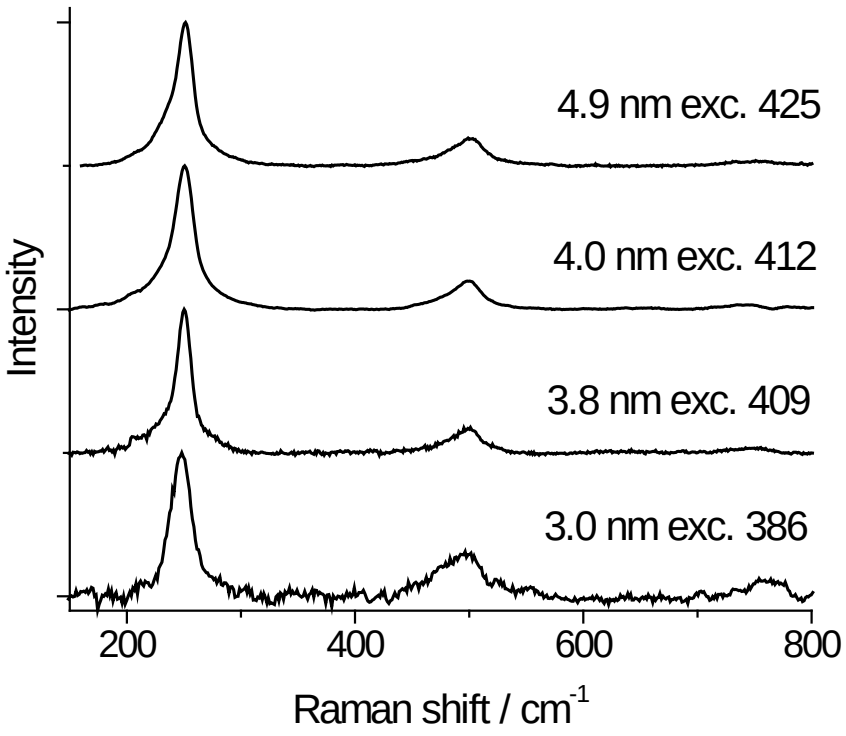

Figure 3. Resonance Raman spectra of ZnSe QDs as dried films. Excitation wavelengths are indicated. Spectra are scaled to a common maximum and displaced vertically.

Table 1. Summary of resonance Raman data for ZnSe quantum dots.

Exc. peak / nm	379		403		406		417	
Diam. / nm	3.0		3.8		4.0		4.9	
Exc. wave / nm	382.3	385.9	400.2	409.1	403.7	412.5	418.2	425.1
$\left(\frac{d\sigma}{d\Omega}\right)_{LO}$ / Å^2 sr^{-1}	---	---	2.33 x 10^{-6}	1.89 x 10^{-6}	4.54 x 10^{-6}	1.53 x 10^{-6}	1.12 x 10^{-5}	6.05 x 10^{-6}
LO depol. ratio	---	---	0.21	0.17	0.20	0.19	0.21	0.20
2LO/LO intensity ratio	0.69	0.56	0.49	0.28	0.42	0.23	0.46	0.31

C. Modeling the spectra to determine Huang-Rhys parameters

While the overtone to fundamental intensity ratio by itself provides a qualitative estimate of the electron-phonon coupling strength, this ratio is also influenced by the degree of electronic resonance, contributions from multiple resonant transitions, and the homogeneous linewidth for the resonant electronic transition(s).[17] For this reason, quantitative determination of the Huang-Rhys parameter (S) requires simulation of the absorption spectrum and Raman intensities with a model that includes S as an adjustable parameter. This was carried out as described previously for CdSe,[5,14] with a few modifications. As with CdSe, the ZnSe absorption spectrum was modeled using five excitonic transitions, four of which were split into a lower-energy (x,y)-polarized component and a higher-energy z-polarized component. That structure was chosen to approximate the splittings of the allowed excitonic transitions in wurtzite CdSe, whereas in zincblende ZnSe QDs the excitonic fine structure will be determined instead by the shape asymmetry. The similarity between the Raman depolarization ratios in wurtzite CdSe and zincblende ZnSe indicate that the effective deviation from spherical symmetry is similar in both systems, and we find that the specific model chosen has little effect on the recovered Huang-Rhys parameters as long as the experimental depolarization ratios are obtained. Also, as we did not obtain Raman data on resonance with the higher-energy transitions in ZnSe, the Huang-Rhys parameters associated with these transitions cannot be determined independently and were set equal to the value used for the lowest excitonic transition with which our laser excitation is resonant. Inclusion of the higher transitions in the model allows us to account for the small preresonant contribution of these transitions at the excitation wavelengths used.

The quantity that we measure is the Raman differential cross section for both parallel and perpendicular polarizations, $\left(\frac{d\sigma}{d\Omega}\right)_{\parallel+\perp}$, in units of Å^2/sr. The cross section for a resonance Raman transition between vibrational states *i* and *f*, as a function of polarization, are calculated as

$$\left(\frac{d\sigma}{d\Omega}\right)_{\parallel} = \frac{\omega_L \omega_S^3}{16\pi^2\hbar^2 c^4 \varepsilon_0^2}\frac{1}{15}\left[8\left|\alpha_{xx,if}\right|^2 + 3\left|\alpha_{zz,if}\right|^2 + 4Re\left(\alpha_{xx,if}^* \alpha_{zz,if}\right)\right] \quad (1)$$

$$\left(\frac{d\sigma}{d\Omega}\right)_{\perp} = \frac{\omega_L \omega_S^3}{16\pi^2\hbar^2 c^4 \varepsilon_0^2}\frac{1}{15}\left[\left|\alpha_{xx,if}\right|^2 + \left|\alpha_{zz,if}\right|^2 - 2Re\left(\alpha_{xx,if}^* \alpha_{zz,if}\right)\right] \quad (2)$$

where ω_L and ω_S are the laser and scattered frequencies. The components of the Raman polarizability tensor are calculated as

$$\alpha_{kk,if} = \sum_e M_{e,k}^2 \int_0^\infty dt\, \langle f|i(t)\rangle_e\, exp\left[i\left(\omega_L - \omega_{eg} + \omega_i\right)t - g_e(t)\right] \quad (3)$$

where *e* is an electronic (electron-hole) state, $M_{e,k}$is the electronic transition dipole moment between the ground state and excited state *e* along direction *k*, ω_{eg} is the frequency difference between the purely electronic states, and $g_e(t)$ is a damping function that accounts for all sources of electronic homogeneous dephasing. The quantity $\langle f|i(t)\rangle_e$ represents the initial ground-state vibrational wavefunction propagated on the excited-state potential energy surface for excitonic state *e*, and this is the quantity that depends on the Huang-Rhys parameter S. Refs. 5 and 14 provide a detailed discussion of the interpretation and implementation of these equations.

Table 2 gives the key parameters for the three larger sizes of ZnSe QDs and Figure 4 shows the calculated and experimental absorption spectra, LO fundamental resonance Raman cross-sections and depolarization ratios, and LO overtone to fundamental intensity ratios for one of the samples. Corresponding plots for the other two sizes, and the complete set of modeling parameters, can be found in the Supporting Information. As stated above, no modeling was

carried out on the smallest QDs because reliable molar absorptivities and absolute cross-section data could not be obtained.

Table 2. Huang-Rhys parameter, electronic homogeneous linewidth, electronic inhomogeneous broadening standard deviation, transition dipole length, and fine-structure splitting used in modeling Raman data of ZnSe quantum dots. See ref. 14 for a description of the parameters.

Size (nm)/wavelength (nm)	4.9/417	4.0/406	3.8/402
Huang-Rhys parameter	0.32	0.32	0.50
Homogeneous width / cm^{-1}	250	320	400
Inhomogeneous std. dev. / cm^{-1}	310	340	280
Transition length / Å	2.09	1.76	1.66
Fine-structure splitting / cm^{-1}	245	275	320

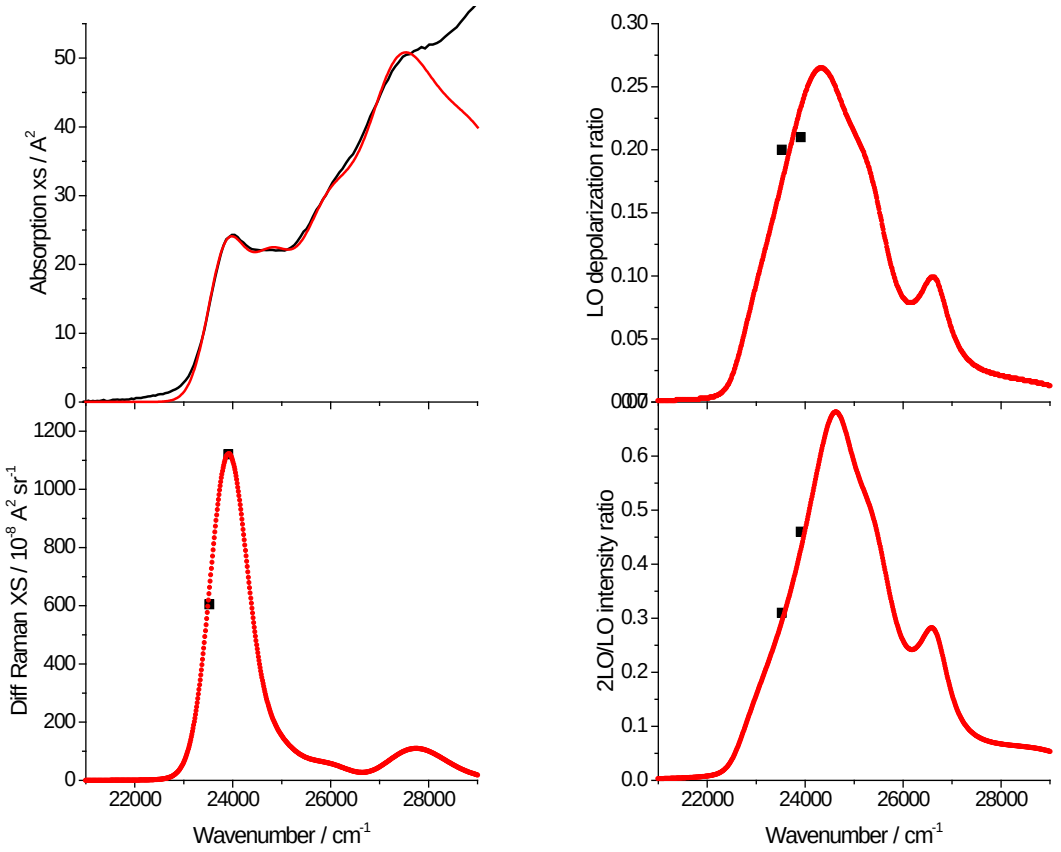

Figure 4. Calculated (red) and experimental (black) absorption cross-section, resonance Raman differential cross-section for the LO phonon, Raman depolarization ratio for the LO phonon, and LO phonon overtone to fundamental intensity ratio for the 4.9 nm diameter ZnSe QDs.

Discussion

Our group has previously utilized quantitative resonance Raman intensity analysis to examine EPC in CdSe QDs as a function of size[5] and in CdSe/CdS core/shell structures.[6] In neither case were the results consistent with expectations based on the Fröhlich mechanism for EPC and an effective mass approximation envelope function model for the electron and hole wavefunctions. The expectation is that EPC should increase as the electron and hole

wavefunctions become more spatially separated, producing a larger electric field that can couple to the polar phonons. The electron-hole separation should be greater in small QDs than in larger ones because of the increased tunneling of the electron wavefunction outside the particle in smaller structures. However, we found only a small size dependence of the EPC, with the LO phonon Huang-Rhys parameters ranging from S = 0.24 to 0.18 for diameters between 2.6 and 5.2 nm. Addition of a CdS shell to form a "quasi-type-II" structure, in which the hole wavefunction is localized to the CdSe core and the electron is largely delocalized over both core and shell, is expected to further increase the EPC for the CdSe phonons; instead, it reduces the Huang-Rhys parameter to about 0.125. Clearly, this simple, spherically symmetric model fails to capture some of the important photophysics of these QDs. We speculate that the breakdown of this simple model and the reason that the EPC is somewhat larger in ZnSe is due to the holes being more localized than what is expected from a spherically symmetric EMA model. This localization may be caused by defects and/or surface effects.

The increased overtone intensity in the smallest ZnSe QDs suggests that the size dependence of the EPC strength may be more pronounced than in CdSe and more in line with expectations, but we cannot quantitate the Huang-Rhys factor for these smallest particles. The present result of stronger EPC in ZnSe than in comparably sized CdSe is not easy to explain based on simple models. ZnSe and CdSe are generally quite similar in their structure and in the nature of the lowest excitonic wavefunctions (4s orbitals make up the conduction band in ZnSe compared with 5s orbitals in CdSe), but CdSe is expected to be slightly more ionic than ZnSe,[11,26] which would lead to the prediction of weaker Fröhlich coupling in ZnSe. Note that while our studies were carried out on zincblende ZnSe QDs and on wurtzite CdSe QDs, we have also shown that wurtzite and zincblende CdSe QDs have almost identical resonance Raman spectra.[27]

We have expressed the strength of exciton-phonon coupling to the LO phonon in terms of the Huang-Rhys parameter, S. A quantity of more significance to the photophysics may be the reorganization energy λ, the energy difference between the excitonic state at the vertically excited ground-state geometry and the excitonic state at the relaxed nuclear geometry. For harmonic phonons and linear EPC, which should be a good approximation for these cases of relatively weak EPC, the reorganization energy is given by $\lambda = \hbar\omega S$ where ω is the phonon frequency. As the phonon frequency in ZnSe is ~20% higher than in CdSe, using reorganization energy as the key parameter slightly amplifies the difference between ZnSe and CdSe. The total reorganization energy is a sum over the contributions from each normal mode including the low-frequency acoustic phonons which we do not see directly in our resonance Raman spectra. We have no direct evidence for the EPC in these modes or how it compares between ZnSe and CdSe, although both direct and indirect evidence from other experiments in CdSe indicates that the contributions from acoustic phonons may be significant.[8,28-33] In our modeling the coupling to acoustic phonons appears as part of the electronic homogeneous linewidth, and this quantity has similar values in CdSe and ZnSe, suggesting similar contributions from acoustic phonons to the total reorganization energy.

Although the exciton-phonon coupling is found to be somewhat larger in ZnSe quantum dots than in CdSe, both are in the "weak coupling" range where more than half of the zero-temperature optical absorption or emission intensity goes into the electronic origin. In these pure binary semiconductors the potential experienced by an electron or a hole is essentially the same in every unit cell and spherically symmetric, leading to relatively little charge separation in the excitonic state. The situation may be considerably different in an alloyed QD such as $Cd_xZn_{1-x}Se$ where cadmium ions are randomly substituted for zinc.[34-37] In this case the potentials governing

the electron and hole wavefunctions will be different in different unit cells and nonspherically symmetric, potentially leading to much greater localization of the hole wavefunction in particular, a greater degree of charge separation, and stronger exciton-phonon coupling. Experiments to probe this are underway.

Conclusions

The Huang-Rhys parameter for the longitudinal optical phonon in the lowest excitonic transition of ZnSe quantum dots is 1.5 to 2 times larger than in CdSe QDs of comparable size. Neither this nor prior results on CdSe QDs as a function of size and shell material are readily explained using standard models for the excitonic wavefunctions and the Fröhlich mechanism for exciton-phonon coupling. The simple particle in a sphere envelope function models for the electron and hole wavefunctions may not properly capture local fluctuations in the internal electric fields that couple to the polar phonons.

Acknowledgements

This work was supported by NSF grant CHE-1506803.

Supporting Information

Details of the two methods used to calculate the molar absorptivity, comparison of experimental and simulated absorption and Raman data for the two intermediate sizes of QDs, a complete list of the modeling parameters, and the sizing curve relating ZnSe QD diameter to energy of the lowest excitonic transition. This material is available free of charge via the Internet at http://pubs.acs.org.

References

1. Kelley, A. M. Comparison of Three Empirical Force Fields for Phonon Calculations in CdSe Quantum Dots. *J. Chem. Phys.* **2016**, *144*, 214702.

2. Efros, A. L.; Rosen, M.; Kuno, M.; Nirmal, M.; Norris, D. J.; Bawendi, M. Band-Edge Exciton in Quantum Dots of Semiconductors with a Degenerate Valence Band: Dark and Bright Exciton States. *Phys. Rev. B* **1996**, *54*, 4843-4856.

3. Kelley, A. M. Electron-Phonon Coupling in CdSe Nanocrystals from an Atomistic Phonon Model. *ACS Nano* **2011**, *5*, 5254-5262.

4. Norris, D. J.; Bawendi, M. G. Measurement and Assignment of the Size-Dependent Optical Spectrum in CdSe Quantum Dots. *Phys. Rev. B* **1996**, *53*, 16338-16346.

5. Lin, C.; Gong, K.; Kelley, D. F.; Kelley, A. M. Size Dependent Exciton-Phonon Coupling in CdSe Nanocrystals through Resonance Raman Excitation Profile Analysis. *J. Phys. Chem. C* **2015**, *119*, 7491-7498.

6. Lin, C.; Gong, K.; Kelley, D. F.; Kelley, A. M. Electron-Phonon Coupling in CdSe/CdS Core-Shell Quantum Dots. *ACS Nano* **2015**, *9*, 8131-8141.

7. Norris, D. J.; Efros, A. L.; Rosen, M.; Bawendi, M. G. Size Dependence of Exciton Fine Structure in CdSe Quantum Dots. *Phys. Rev. B* **1996**, *53*, 16347-16354.

8. Eilers, J.; van Hest, J.; Meijerink, A.; de Mello Donega, C. Unravelling the Size and Temperature Dependence of Exciton Lifetimes in Colloidal ZnSe Quantum Dots. *J. Phys. Chem. C* **2014**, *118*, 23313−23319.

9. Hennion, B.; Moussa, F.; Pepy, G.; Kunc, K. Normal Modes of Vibration in ZnSe. *Phys. Lett.* **1971**, *36A*, 376-378.

10. Widulle, F.; Kramp, S.; Pyka, N. M.; Gobel, A.; Ruf, T.; Debernardi, A.; Lauck, R.; Cardona, M. The Phonon Dispersion of Wurtzite CdSe. *Physica B* **1999**, *263-264*, 448-451.

11. Berlincourt, D.; Jaffe, H.; Shiozawa, L. R. Electroelastic Properties of the Sulfides, Selenides, and Tellurides of Zinc and Cadmium. *Phys. Rev.* **1963**, *129*, 1009-1017.

12. Islam, S. K.; Lombardi, J. R. Enhancement of Surface Phonon Modes in the Raman Spectrum of ZnSe Nanoparticles on Adsorption of 4-Mercaptopyridine. *J. Chem. Phys.* **2014**, *140*, 074701.

13. Kumar, P.; Singh, J.; Pandey, M. K.; Jeyanthi, C. E.; Siddheswaran, R.; Paulraj, M.; Hui, K. N.; Hui, K. S. Synthesis, Structural, Optical and Raman Studies of Pure and Lanthanum Doped ZnSe Nanoparticles. *Mat. Res. Bull.* **2013**, *49*, 144-150.

14. Baker, J. A.; Kelley, D. F.; Kelley, A. M. Resonance Raman and Photoluminescence Excitation Profiles and Excited-State Dynamics in CdSe Nanocrystals. *J. Chem. Phys.* **2013**, *139*, 024702.

15. Pu, C.; Zhou, J.; Lai, R.; Niu, Y.; Nan, W.; Peng, X. Highly Reactive, Flexible yet Green Se Precursor for Metal Selenide Nanocrystals: Se–Octadecene Suspension (Se–Sus). *Nano Res.* **2013**, *6*, 652-670.

16. Trulson, M. O.; Mathies, R. A. Raman Cross Section Measurements in the Visible and Ultraviolet Using an Integrating Cavity: Application to Benzene, Cyclohexane, and Cacodylate. *J. Chem. Phys.* **1986**, *84*, 2068-2074.

17. Kelley, A. M. Resonance Raman Overtone Intensities and Electron-Phonon Coupling Strengths in Semiconductor Nanocrystals. *J. Phys. Chem. A* **2013**, *117*, 6143-6149.

18. Myers, A. B. Excited Electronic State Properties from Ground-State Resonance Raman Intensities. In *Laser Techniques in Chemistry*; Myers, A. B., Rizzo, T. R., Eds.; Wiley: New York, 1995; pp 325-384.

19. Myers, A. B. Molecular Electronic Spectral Broadening in Liquids and Glasses. *Ann. Rev. Phys. Chem.* **1998**, *49*, 267-295.

20. Jasieniak, J.; Smith, L.; van Embden, J.; Mulvaney, P.; Califano, M. Re-Examination of the Size-Dependent Absorption Properties of CdSe Quantum Dots. *J. Phys. Chem. C* **2009**, *113*, 19468-19474.

21. Capek, R. K.; Moreels, I.; Lambert, K.; De Muynck, D.; Zhao, Q.; Van Tomme, A.; Vanhaecke, F.; Hens, Z. Optical Properties of Zincblende Cadmium Selenide Quantum Dots. *J. Phys. Chem. C* **2010**, *114*, 6371-6376.

22. Giblin, J.; Kuno, M. Nanostructure Absorption: A Comparative Study of Nanowire and Colloidal Quantum Dot Absorption Cross Sections. *J. Phys. Chem. Lett.* **2010**, *1*, 3340-3348.

23. Nikesh, V. V.; Lad, A. D.; Kimura, S.; Nozaki, S.; Mahamuni, S. Electron Energy Levels in ZnSe Quantum Dots. *J. Appl. Phys.* **2006**, *100*, 113520.

24. Lin, C.; Kelley, D. F.; Rico, M.; Kelley, A. M. The "Surface Optical" Phonon in CdSe Nanocrystals. *ACS Nano* **2014**, *8*, 3928-3938.

25. Dzhagan, V. M.; Valakh, M. Y.; Raevskaya, A. E.; Stroyuk, A. L.; Kuchmiy, S. Y.; Zahn, D. R. T. Size Effects on Raman Spectra of Small CdSe Nanoparticles in Polymer Films. *Nanotechnology* **2008**, *19*, 305707.

26. Christensen, N. E.; Satpathy, S.; Pawlowska, Z. Bonding and Ionicity in Semiconductors. *Phys. Rev. B* **1987**, *36*, 1032-1050.

27. Kelley, A. M.; Dai, Q.; Jiang, Z.; Baker, J. A.; Kelley, D. F. Resonance Raman Spectra of Wurtzite and Zincblende CdSe Nanocrystals. *Chem. Phys.* **2013**, *422*, 272-276.

28. Werschler, F.; Hinz, C.; Froning, F.; Gumbsheimer, P.; Haase, J.; Negele, C.; de Roo, T.; Mecking, S.; Leitenstorfer, A.; Seletskiy, D. V. Coupling of Excitons and Discrete Acoustic Phonons in Vibrationally Isolated Quantum Emitters. *Nano Lett.* **2016**, *16*, 5861−5865.

29. Oron, D.; Aharoni, A.; de Mello Donega, C.; van Rijssel, J.; Meijerink, A.; Banin, U. Universal Role of Discrete Acoustic Phonons in the Low Temperature Optical Emission of Colloidal Quantum Dots. *Phys. Rev. Lett.* **2009**, *102*, 177402.

30. Sagar, D. M.; Cooney, R. R.; Sewall, S. L.; Dias, E. A.; Barsan, M. M.; Butler, I. S.; Kambhampati, P. Size Dependent, State-Resolved Studies of Exciton-Phonon Couplings in Strongly Confined Semiconductor Quantum Dots. *Phys. Rev. B* **2008**, *77*, 235321.

31. Sagar, D. M.; Cooney, R. R.; Sewall, S. L.; Kambhampati, P. State-Resolved Exciton-Phonon Couplings in CdSe Semiconductor Quantum Dots. *J. Phys. Chem. C* **2008**, *112*, 9124-9127.

32. Fernée, M. J.; Littleton, B. N.; Cooper, S.; Rubinsztein-Dunlop, H.; Gomez, D. E.; Mulvaney, P. Acoustic Phonon Contributions to the Emission Spectrum of Single CdSe Nanocrystals. *J. Phys. Chem. C* **2008**, *112*, 1878-1884.

33. Salvador, M. R.; Graham, M. W.; Scholes, G. D. Exciton-Phonon Coupling and Disorder in the Excited States of CdSe Colloidal Quantum Dots. *J. Chem. Phys.* **2006**, *125*, 184709.

34. Groeneveld, E.; Witteman, L.; Lefferts, M.; Ke, X.; Bals, S.; Van Tendeloo, G.; de Mello Donega, C. Tailoring ZnSe-CdSe Colloidal Quantum Dots Via Cation Exchange: From Core/Shell to Alloy Nanocrystals. *ACS Nano* **2013**, *7*, 7913-7930.

35. Zhong, X.; Han, M.; Dong, Z.; White, T. J.; Knoll, W. Composition-Tunable $Zn_xSd_{1-X}Se$ Nanocrystals with High Luminescence and Stability. *J. Am. Chem. Soc.* **2003**, *125*, 8589-8594.

36. Beane, G. A.; Gong, K.; Kelley, D. F. Auger and Carrier Trapping Dynamics in Core/Shell Quantum Dots Having Sharp and Alloyed Interfaces. *ACS Nano* **2016**, *10*, 3755-3765.

37. Acharya, K. P.; Nguyen, H. M.; Paulite, M.; Piryatinski, A.; Zhang, J.; Casson, J. L.; Xu, H.; Htoon, H.; Hollingsworth, J. A. Elucidation of Two Giants: Challenges to Thick-Shell Synthesis in CdSe/ZnSe and ZnSe/CdS Core/Shell Quantum Dots. *J. Am. Chem. Soc.* **2015**, *137*, 3755-3758.

Table of Contents graphic